Turbulent rotating disk flow with inward throughflow

By S. PONCET, M. P. CHAUVE and P. LE GAL

IRPHE, UMR 6594, CNRS – Université d'Aix-Marseille I & II,
Technopôle Château-Gombert, 49, rue F. Joliot-Curie, 13384 Marseille cédex 13, France

The evolution of the entrainment coefficient K of the rotating fluid in a rotor–stator cavity with an inward throughflow and pre-rotation is studied according to the flow parameters. Measurements are obtained in water for a turbulent Batchelor type of flow with two separated boundary layers on the rotating and stationary disks by means of a laser Doppler anemometer, and the results are compared to those performed using pressure transducers. We show that the entrainment coefficient K depends on a local flow rate coefficient Cq_r according to a 5/7 power law whose coefficients depend on the boundary conditions. A theoretical analysis confirms this behaviour of K.

1. Introduction

Stépanoff (1932) was the first to determine the ratio K between the mean azimuthal velocity V_θ of the turbulent flow in a rotor–stator cavity, and that of the disk Ωr at the same radius, where Ω is the angular velocity of the rotating disk and r the local radius. He suggested a value of K equal to 0.5 and independent of the radial location. Then Schultz-Grunow (1935) proposed a flow pattern divided into three layers: two of them localized in the vicinities of the walls and a third one, the core, located between them. He calculated a theoretical value of $K = V_\theta/\Omega r = 0.512$, in the core and measured an experimental value equal to 0.357. He interpreted this discrepancy as due to the existence of a shear stress in the small radial gap between the rotating disk and the fixed cylindrical endwall. Batchelor (1951) performed a similarity analysis by solving the system of differential equations relating to the stationary axisymmetric flow between two infinite disks. He also specified the formation of a non-viscous core in solid-body rotation confined between the two boundary layers, which develop on the disks.

This division of the flow into three distinct zones was the subject of an intense controversy: Stewartson (1953) found that the tangential velocity of the fluid can indeed be zero everywhere apart from the rotor boundary layer. Kreiss & Parter (1983) finally proved the existence of a multiple class of solutions discovered numerically by Mellor, Chapple & Stokes (1968). Daily & Nece (1960) studied the effects of the disk speed and of the inter-disk gap h on the structure of the turbulent flow using pressure and velocity measurements. They proposed constant values of K along a radius and found that K is sensitive to variations of h. Cooper & Reshotko (1975) found that K tends to 0.5 in the case of a turbulent flow between a stationary and a rotating disk of infinite radius. In the 1980s, Szeri *et al.* (1983) studied the flow in a rotor–stator system with a large radial gap and showed that the value 0.313 is a good estimation of K for $0.3 < r/R_2 < 0.5$ (r/R_2 is the ratio between the local radius

and the rotating disk radius) and that for greater radius, K is an increasing function of r. The measurements performed by Dijkstra & van Heijst (1983) extended the self-similar flow area for all radii lower than 0.75 and also showed that K depends strongly on the radial position beyond this radius. Adding a flow pre-rotation equal to the disk velocity at the periphery, made the radial dependence of K much stronger. Thus, it appears that the evolution of the entrainment coefficient K of the rotating fluid along the radius is strongly influenced by the boundary conditions.

Lance & Rogers (1962) showed numerically that closed or partially closed inter-disk flows can be classified into two families according to the inter-disk gap h. Sirivat (1991) and then Schouveiler, Le Gal & Chauve (2001) confirmed this classification by their experimental contributions. When h is larger than the boundary layer thicknesses, the boundary layers are separated, and the averaged flow is classically separated into three zones and belongs to the Batchelor-type family. The first zone is related to the boundary layer developed on the fixed disk: it is called the Bödewadt layer. The tangential velocity of the flow varies between $K\Omega r$ in the core to zero on the stationary disk. Note that this Bödewadt layer is highly unstable and was the subject of several detailed studies by Savas (1987), Lopez (1998), Schouveiler *et al.* (1999) and Gauthier, Gondret & Rabaud (1999). The second zone is defined by a tangential speed equal to $K\Omega r$ and a quasi-zero radial velocity: the core. The third zone is associated with the boundary layer which develops on the rotor: it is the von Kármán or Ekman layer. In this zone, the tangential velocity varies from Ωr on the rotating disk to that of the core, $K\Omega r$.

For the case when a radial inflow or outflow is imposed, fewer results have been published. Daily, Ernst & Asbedian (1964) measured the average velocity profiles in the case of rotor–stator systems with an imposed outward throughflow and found the same classification as specified by Owens & Rogers (1989) in the case of closed flows. They also proposed a qualitative representation of the average pseudo-streamlines that they observed from their numerical simulations. They showed that, in the case of a turbulent Batchelor flow with a weak throughflow, the flow at the periphery keeps the same properties as the flow without flux with the flux passing through the Bödewadt layer and compressing the core. When approaching the centre of the disk, the Ekman layer, which was centrifugal, becomes centripetal at a certain radius. A stagnation line is thus created on the rotor. It is similar to that observed by Dijkstra & van Heijst (1983). With a strong centripetal flow, both boundary layers are centripetal. Kurokawa & Toyokura (1972) proposed a one-dimensional model to calculate K and introduced a global coefficient of throughflow rate. They validated their model by experimental measurements and showed the dominating influence of a centripetal flow in the determination of K and on the distribution of pressure along the radius. But their model remains complex and difficult to use. Debuchy (1993) performed a comparative study between experimental results on a rotating centripetal flow and computations obtained with a numerical model developed from an asymptotic approach. But the limitations inherent to the turbulence models and to the representations of the boundary conditions do not allow reliable predictions to be obtained. Later Elena & Schiestel (1995) proposed some numerical calculations of turbulent rotating flows based on the use of a new modelling of the Reynolds stress tensors. But there also, the authors note the too high laminarization of the flow in comparison with the known results.

The interest in this kind of flow is wide. Of course it is of major interest in turbomachinery, but examples where rotation and throughflow are associated can also be found in geophysics or astrophysics. Moreover, from a fundamental point of view, the rotor–stator problem is one of the simplest configuration where exact solutions of the
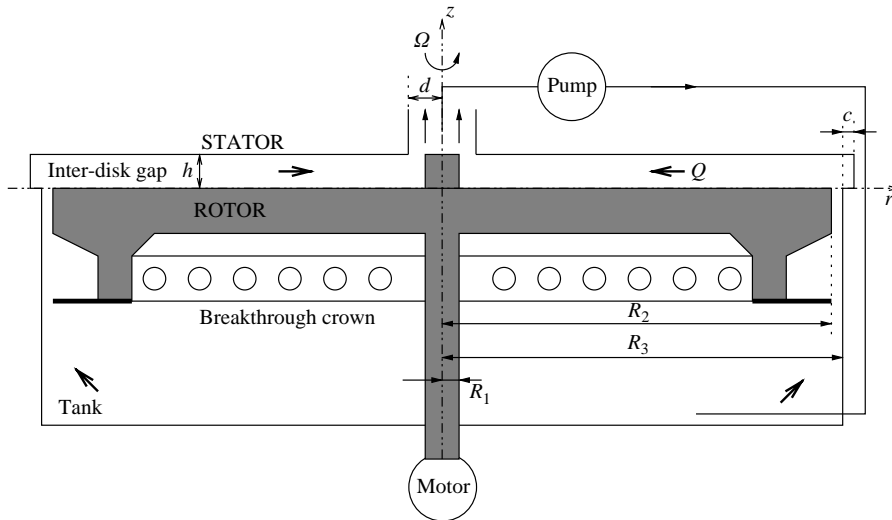
FIGURE 1. Schematic representation of the experimental set-up and notation. $d = 55$ mm is the radius of the central opening, $R_1 = 38$ mm and $R_2 = 250$ mm are the inner and outer radii of the rotating disk and $R_3 = 253$ mm is the outer radius of the cavity whose height h can be adjusted between 0 and 12 mm. The groove depth c is fixed to 5 mm.

Navier–Stokes equations can be found and where rotation influences turbulence modelling: this is the reason why they have often become benchmarks for numerical simulations.

Our present study relates to the determination of K when a centripetal flux is added to the turbulent rotating fluid. Following the analysis performed by Gassiat (2000), we show that a local flow rate coefficient Cq_r is the similarity parameter of the flow that can be used directly to calculate the entrainment coefficient K of the fluid. As these values are connected to the pressure gradient across the cavity, a comparison between velocity and pressure measurements is performed. The paper is divided as follows: § 2 is the description of the experimental set-up whereas § 3 is devoted to the analytical model that we have deduced from friction considerations. This analysis leads to the determination of the behaviour of K versus Cq_r. In § 4, the experimental results are presented and discussed before concluding in § 5.

2. Experimental set-up

The geometrical characteristics of our rotating disk cavity are displayed in figure 1. It consists of a cylindrical cavity enclosed by a fixed disk (the stator) and a smooth rotating disk (the rotor). A fixed shroud surrounds the cavity. The rotor and the central hub attached to it rotate at the constant angular velocity Ω.

The flow depends mainly on three control parameters: the aspect ratio G, the global Reynolds number Re_{R_2} and the dimensionless flow rate Q^* defined as follows: $G = h/R_2$, $Re_{R_2} = \Omega R_2^2/\nu$, $Q^* = Q/(\nu R_2)$, where ν is the kinematic viscosity of water, R_2 the rotating disk radius and Q the throughflow rate. The height of the cavity h is variable between 0 and 12 mm. The radial gap $e = R_3 - R_2$ is fixed to 3 mm (R_3 is the outer radius of the cylindrical housing). As the disk rotates, water is sucked through the central opening of the cavity situated above the hub, with radius d equal to 55 mm. The incoming fluid is entrained into rotation while passing through a

breakthrough crown mounted underneath the rotor and linked to it, which enables an increase of the tangential velocity of the fluid, and consequently limits the influence of the non-rotating cylindrical wall. This pre-rotation is achieved through 48 holes having a diameter of 10 mm calibrated in order to entrain enough fluid when the disk rotates. It ranges between 0.43 and 0.5 for the considered values of the flow control parameters. A pump allows a centripetal and variable flux Q to be imposed. The measurement of the flow rate is performed by an electromagnetic flow-meter, located at the exit of the cavity. The rotation of the disk is provided by a 5.5 KW electric servo-motor. A variable-speed numerical controller controls the angular velocity Ω. The precision on the measurement of the angular velocity and on the flux is better than 1%. In order to avoid cavitation effects, the cavity is maintained at a pressure of 2 bars. Pressurization is ensured by a tank-buffer and is controlled by two pressure gauges. The temperature is also maintained constant (23 °C) by a special water cooling device in order to keep the density and the kinematic viscosity of water constant. The measurements are performed by means of a laser Doppler anemometer (LDA) from the Dantec company and also by pressure transducers. The LDA technique is used to measure the tangential velocity in the vertical plane (r, z) at a given azimuthal angle. The main defect of this non-intrusive method is due to the size of the probe volume (0.8 mm in the axial direction) that alters the quality of the velocity field measurements in the boundary layers. Pressure is measured by six piezoresistive transducers. These transducers are highly accurate (0.05% in the range 10 °C to 40 °C) and combine both pressure sensors and electronic temperature compensations. They are fixed to the stator at the radial positions 0.093, 0.11, 0.14, 0.17, 0.2 and 0.23 m located on two rays. Previous pressure measurements by embeded pressure gauges (Gassiat 2000) showed that the pressures on the rotor and on the stator are the same within 2.5%. This is a direct consequence of the Taylor–Proudman theorem, which forbids axial gradients in fast rotating flows.

3. Analytical model

3.1. *Governing equations*

The turbulent flow is governed by the Navier–Stokes equations written in cylindrical coordinates (r, θ, z). We denote the components of the velocity field (V_r, V_θ, V_z) and the pressure P. As we saw previously, for large h compared to the boundary layer thicknesses, the mean flow is of Batchelor type with a central core and two boundary layers (Daily & Nece 1960). The aim of our analysis is to describe the flow in the central core. In this region, it is well known that $V_r \simeq V_z \simeq 0$ (see Kurokawa & Toyokura 1972). Moreover, the tangential velocity remains constant along the z-axis and so depends only on the radial position (see figure 2). Thus, it appears that all the flux passing through the cavity is confined in the boundary layers. So the Navier–Stokes equation for the tangential component reduces to the balance of the centrifugal force and the radial pressure gradient: $\rho V_\theta^2 / r = \partial P / \partial r$. Then, if we define the following dimensionless quantities: $r^* = r/R_2$, $P^* = P/(1/2\rho(\Omega R_2)^2)$, we obtain $dP^*/dr^* = 2K^2 r^*$. The reference pressure is measured at the outer radial position $r^* = 0.92$. Thus, we define a pressure coefficient, as follows: $C_p(r^*) = P^*(r^*) - P^*(r^* = 0.92)$. Finally the resulting equation that will allow a comparison between the pressure field and the velocity field is

$$\mathrm{d}C_p(r^*)/\mathrm{d}r^* = 2K^2 r^*. \tag{3.1}$$

3.2. *Definition of the local flow rate coefficient Cq_r*

The challenge is to find an equation linking the rate of rotation of the fluid K to h, Ω and Q. It is recalled that we consider a flow with two turbulent boundary layers separated by a central rotating core. First we seek an expression for the thickness of the Ekman layer δ_E. Following the analysis of Schlichting (1979), we assume that the velocity profiles evolve according to the classical one-seventh power law in the boundary layers. Thus, the friction coefficient Cf, equal by definition to the normalized shear stress τ_0, can be given by Dean's formula (Nakabayashi, Kitoh & Katoh 2004): $Cf_{mean} = 0.073\,Re_{mean}^{-1/4}$, where Re_{mean} is the Reynolds number based on U_{mean}, the mean velocity at the cross-section. In our case, we take the mean tangential velocity in the Ekman layer to be $U_{mean} = (K+1)\Omega r/2$ and the characteristic length to be the Ekman layer thickness δ_E. Thus, the friction coefficient is given by

$$Cf \sim \left(\frac{K+1}{2}\Omega r\right)^{-1/4}\left(\frac{\delta_E}{\nu}\right)^{-1/4}. \tag{3.2}$$

By denoting the angle formed by the shear stress at the wall as α and the tangential direction as τ_0, the tangential component is expressed by

$$\tau_0^\theta = \tau_0\cos\alpha \sim \rho\left(\frac{K+1}{2}\Omega r\right)^{7/4}\left(\frac{\nu}{\delta_E}\right)^{1/4}. \tag{3.3}$$

The radial component of the shear stress is obtained by the balance between the centrifugal force and the shear stress in a volume element having a height equal to δ_E:

$$\tau_0^r = \tau_0\sin\alpha = \rho\Omega^2 r\delta_E. \tag{3.4}$$

As the angle α of streamline inclination remains constant along the radius r (experimentally verified), we find the following expression for the Ekman layer thickness:

$$\delta_E \sim r\left(\frac{K+1}{2}\right)^{7/5}\left(\frac{\Omega r^2}{\nu}\right)^{-1/5}. \tag{3.5}$$

Secondly, we suppose that the radial friction in the Bödewadt boundary layer is controlled by the radial flux Q_B, with $Q_B < 0$. Now, by considering that the radial velocity in the rotating core is zero, the continuity equation is

$$\overline{V_E}\delta_E = \frac{Q_t - Q_B}{2\pi r}. \tag{3.6}$$

Q_t is the total superimposed flux. $\overline{V_E}$ is a bulk velocity in the Ekman layer, proportional to the maximum value of the velocity reached in this layer, with the proportionality coefficient β: $\overline{V_E} = \beta\Omega r$. Using (3.6) and the expression for $\overline{V_E}$, we finally obtain

$$K = 2\left(\frac{Re_r^{1/5}}{\beta 2\pi r^3\Omega}(Q_t - Q_B)\right)^{5/7} - 1, \tag{3.7}$$

with the expression for the new similarity parameter $Cq_r = Q_t Re_r^{1/5}/(2\pi r^3\Omega)$, where $Re_r = \Omega r^2/\nu$ is the local Reynolds number. The final expression is then
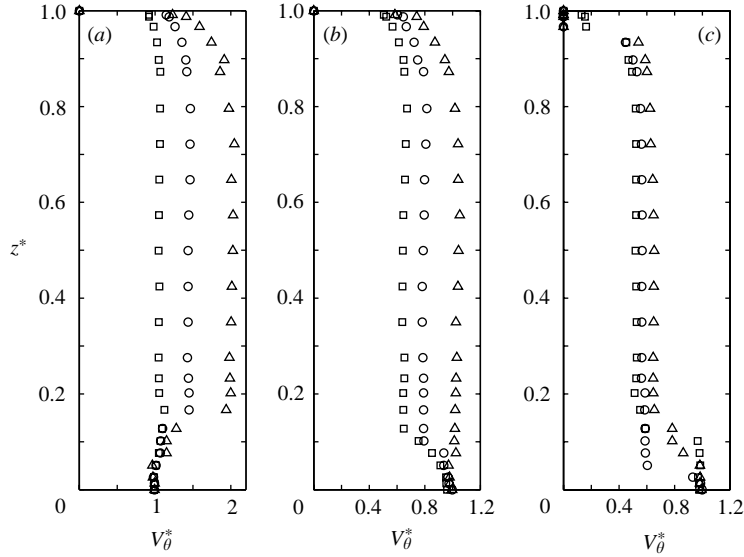
$$K = 2\times(a\times Cq_r + b)^{5/7} - 1 \tag{3.8}$$

FIGURE 2. Influence of the Reynolds number on the axial profiles of the dimensionless tangential velocity for $G = 0.048$ and $Q^* = 10317$: $\triangle$, $Re_{R_2} = 1.038 \times 10^6$; $\circ$, $Re_{R_2} = 2.076 \times 10^6$; $\square$, $Re_{R_2} = 4.151 \times 10^6$: (a) $r^* = 0.44$, (b) $r^* = 0.68$, (c) $r^* = 0.98$.

with a and b two experimental constants; b is obtained from the case without flux $Q_t = 0$. Note that, for $r = R_2$, the expression for Cq_r is the same as in Kurokawa & Toyokura (1972).

4. Experimental results

4.1. *Velocity profiles*

Figure 2 presents axial profiles of the dimensionless tangential velocity $V_\theta^* = V_\theta / \Omega r$ for various experimental configurations. We analyse the influence of the radial position, and of the Reynolds number, for a given aspect ratio $G = 0.048$ and a flow rate $Q^* = 10317$. In each case, the existence of the three characteristic zones: the two boundary layers and the rotating core, is confirmed. Moreover, between $r^* = 0.44$ and 0.68, the flow is approximatively self-similar. However, as can be observed on figure 2, K increases close to the centre because of the conservation of the angular momentum. In particular, for $r^* = 0.44$, K can be greater than one. This means that the fluid rotates faster than the disk and consequently the Ekman layer becomes centripetal. Note that unlike the contra-rotating disks experiments of Lopez *et al.* (2002) or Moisy *et al.* (2004), no inner shear layer is attached to the stagnation point, as in our experiment, the vorticity profiles do not exhibit a local maximum. Closer to the periphery, at $r^* = 0.98$, the flow is strongly influenced by the boundary conditions. The influence of the local Reynolds number and of the dimensionless flow rate Q^* on the tangential velocity is presented in figure 3 for $G = 0.036$. For $Q^* = 10317$ and a given radius $r^* = 0.68$, the dimensionless tangential velocity in the core K decreases for increasing values of Re_{R_2}. On the other hand, for $Re_{R_2} = 1.038 \times 10^6$, at a given radius $r^* = 0.56$, K increases for increasing values of Q^*. Measurements have been obtained for G equal to 0.024, 0.036 and 0.048 and compared in figure 4 for $Re_{R_2} = 4.15 \times 10^6$
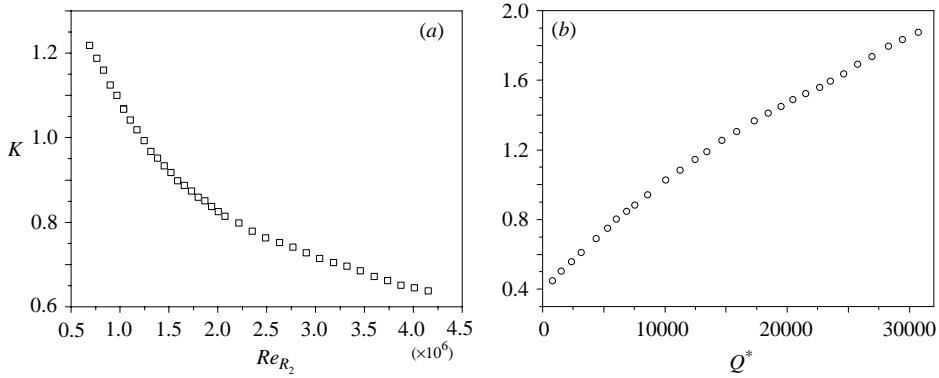
FIGURE 3. Evolution of K with (a) Re_{R_2}, for $G = 0.036$, $Q^* = 10317$ and $r^* = 0.68$, (b) Q^*, for $G = 0.036$, $Re_{R_2} = 1.038 \times 10^6$ and $r^* = 0.56$.
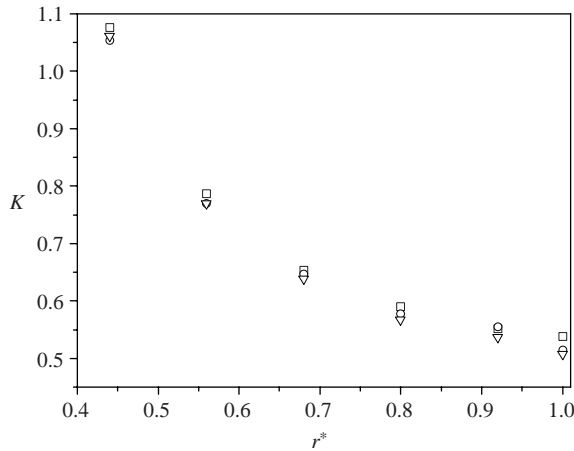

FIGURE 4. Radial evolution of K for $Re_{R_2} = 4.15 \times 10^6$ and $Q^* = 10317$ for different values of G: $\square$, $G = 0.024$; $\circ$, $G = 0.036$; $\triangledown$, $G = 0.048$.

and $Q^* = 10317$, where it is clearly seen that K is not sensitive to such variations of G, as the flows remain in the same regime (turbulent with separated boundary layers).

4.2. Pressure distributions

To complete the experimental analysis of the flow, we also performed pressure measurements by means of six pressure transducers, located on the stator on two rays because of geometrical constraints. In figure 5(a), we plot the coefficient C_p versus r^* for few relevant cases. As expected, the pressure decreases towards the centre of the cavity: C_p is thus always negative. Moreover, at a given radial position and for a given angular velocity, it can be observed that C_p decreases for increasing values of the flow rate Q^*. On the other hand, for a given value of Q^*, C_p increases for increasing values of Re_{R_2}.

According to relation (3.1), we can determine the entrainment coefficient K from the value of C_p. To calculate the derivative of C_p, it is first necessary to perform a polynomial fit of the curves C_p versus r^*. Then, we calculate by finite difference the derivative of C_p in order to obtain the value of K. Figure 5(b) compares the variations of K with the dimensionless radius r^* for the data series obtained by the pressure
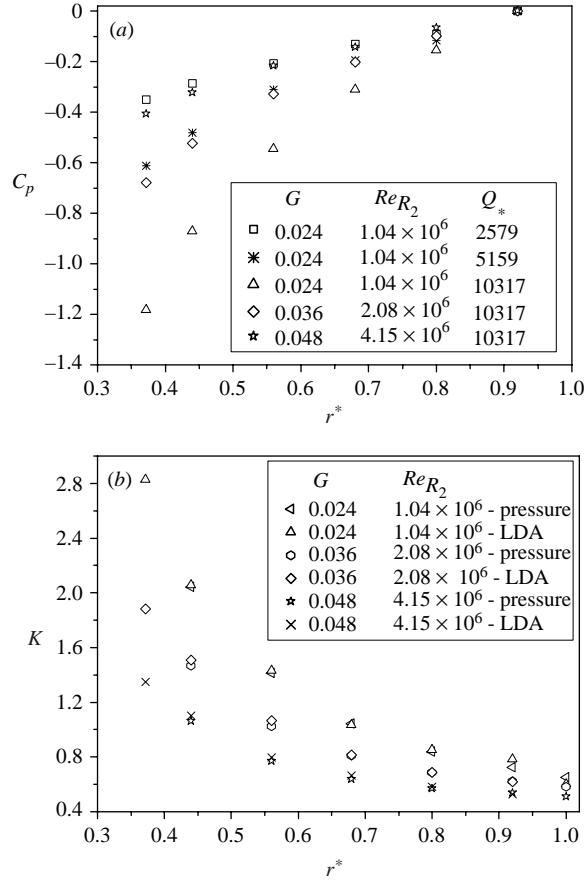
FIGURE 5. (*a*) Radial distributions of the pressure coefficient C_p for various flow conditions. (*b*) Radial profiles of K: comparison between the values of K obtained from the pressure measurements and from laser anemometry, for various flow conditions ($Q^* = 10317$).

sensors and from the LDA measurements. The results are in excellent agreement. The small differences come from the calculation of the derivative of the coefficient C_p.

4.3. 5/7 *power law*

Relation (3.8) has been tested for many values of Q, Ω and r and for the three values of the inter-disk gap h. Figure 6 shows that the whole set of experimental results are in very good agreement with a polynomial fit: $K = 2 \times (5.9 \times Cq_r + 0.63)^{5/7} - 1$.

In particular, figure 6 shows that K is independent of the aspect ratio G as three different $G = 0.024, 0.036, 0.048$ configurations have been studied. The explanation of this behaviour comes from the fact that the mean flow remains in each case a Batchelor-type flow with separated turbulent boundary layers. The 5/7 law has also been validated in the range of Reynolds numbers $[6.92 \times 10^5 - 4.15 \times 10^6]$ and of flow rates $[1247 - 18215]$. Because of experimental constraints, it was not possible to obtain a value of Cq_r greater than 0.2 while keeping the boundary layers turbulent.

For low flux and rather large radius (small values of Cq_r), the flow tends to a self-similar Batchelor-type flow, where the entrainment coefficient K is constant. The asymptotical value of K for $Q^* = 0$ is 0.438. This value is higher that the one obtained in the case of a large radial gap ($K = 0.313$, Szeri *et al.* 1983), mainly because of
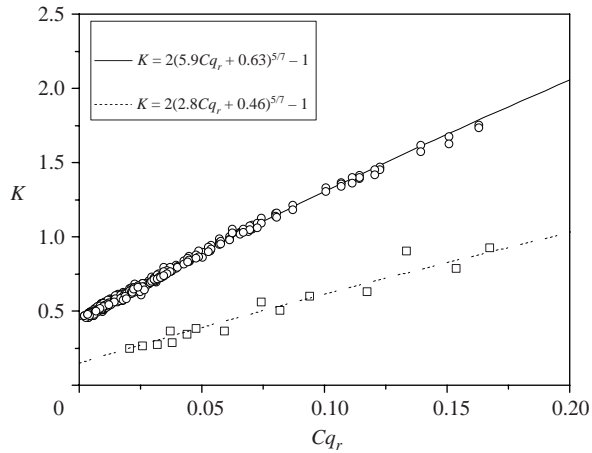
FIGURE 6. 5/7 power law giving K versus Cq_r: $\circ$, present measurements; $\square$, measurements of Debuchy.

the influence of our pre-rotation conditions. On the other hand, on approaching the centre of the disk for strong axial flux, the dependence in the power 5/7 becomes dominant. We also report on figure 6 the velocity measurements of Debuchy (1993) in the case of weak prerotation. As can be seen, these data also follow a 5/7 power law but with smaller coefficients as expected from the absence of pre-rotation in this experiment.

5. Conclusion

We have studied in this experimental work the behaviour of the entrainment co-efficient K of the turbulent flow in a rotor–stator cavity, as a function of the Reynolds number, of the throughflow rate and of the aspect ratio of the cavity. In particular, we determined an analytical law, which enables to calculate the entrainment coefficient K versus a local flow rate coefficient Cq_r. This law has been determined analytically and has been validated by extensive pressure and velocity measurements for different values of the inter-disk gap h and in a large range of Reynolds numbers and flow rates. We have also determined the structure of the rotating-disk flow when an inward flux is added. For a weak throughflow, the flow at the periphery keeps the same pro-perties as the case without flux: the Ekman boundary is centrifugal and the Bödewadt boundary layer is centripetal. These layers are separated by a central rotating core. But, for a strong throughflow, the flow in the Ekman boundary layer becomes centri-petal as the core rotates faster than the rotating disk.

REFERENCES

BATCHELOR, G. K. 1951 Note on a class of solutions of the Navier-Stokes equations representing steady rotationally-symmetric flow. *Q. J. Mech. Appl. Maths* **4**, 29–41.

COOPER, P. & RESHOTKO, E. 1975 Turbulent flow between a rotating disk and a parallel wall. *AIAA J.* **13**, 573–578.

DAILY, J. W., ERNST, W. D. & ASBEDIAN, V. V. 1964 Enclosed rotating disks with superposed throughflow. *Tech. Rep. 64*. MIT, Department of Civil Engineering.

DAILY, J. W. & NECE, R. E. 1960 Chamber dimension effects on induced flow and frictional resistance of enclosed rotating disks. *Trans. ASME: J. Basic Engng* **82**, 217–232.

DEBUCHY, R. 1993 Ecoulement turbulent avec aspiration radiale entre un disque fixe et un disque tournant. PhD thesis, Université des Sciences et Technologies de Lille.

DIJKSTRA, D. & VAN HEIJST, G. J. F. 1983 The flow between two finite rotating disks enclosed by a cylinder. *J. Fluid Mech.* **128**, 123–154.

ELENA, L. & SCHIESTEL, R. 1995 Turbulence modeling of confined flow in rotating disk systems. *AIAA J.* **33**, 812–821.

GASSIAT, R. M. 2000 Etude expérimentale d'écoulements centripètes avec prérotation d'un fluide confiné entre un disque tournant et un carter fixe. PhD thesis, Université de la Méditerranée Aix-Marseille II.

GAUTHIER, G., GONDRET, P. & RABAUD, M. 1999 Axisymmetric propagating vortices in the flow between a stationary and a rotating disk enclosed by a cylinder. *J. Fluid Mech.* **386**, 105–126.

KREISS, H. O. & PARTER, S. V. 1983 On the swirling flow between rotating coaxial disks: existence and uniqueness. *Commun. Pure Appl. Maths* **36**, 55–84.

KUROKAWA, J. & TOYOKURA, T. 1972 Study on axial thrust of radial flow turbomachinery. *2nd Intl JSME Symp. Fluid Machinery and Fluidics, Tokyo, 4–9 September*, vol. 2, p. 31.

LANCE, G. N. & ROGERS, M. H. 1962 The axially symetric flow of a viscous fluid between two infinite rotating disks. *Proc. R. Soc. Lond.* A **266**, 109–121.

LOPEZ, J. M. 1998 Characteristics of endwall and sidewall boundary layers in a rotating cylinder with a differentially rotating endwall. *J. Fluid Mech.* **359**, 49–79.

LOPEZ, J. M., HART, J. E., MARQUES, F., KITTELMAN, S. & SHEN, J. 2002 Instability and mode interactions in a differentially driven rotating cylinder. *J. Fluid Mech.* **462**, 383–409.

MELLOR, G. L., CHAPPLE, P. J. & STOKES, V. K. 1968 On the flow between a rotating and a stationary disk. *J. Fluid Mech.* **31**, 95–112.

MOISY, F., DOARÉ, O., PASUTTO, T., DAUBE, O. & RABAUD, M. 2004 Experimental and numerical study of the shear layer instability between two counter-rotating disks. *J. Fluid Mech.* **507**, 175–202.

NAKABAYASHI, K., KITOH, O. & KATOH, Y. 2004 Similarity laws of velocity profiles and turbulence characteristics of Couette–Poiseuille turbulent flows. *J. Fluid Mech.* **507**, 43–69.

OWENS, J. M. & ROGERS, R. H. 1989 *Flow and Heat Transfer in Rotating-Disc Systems – Vol. 1: Rotor–Stator Systems*. John Wiley and Sons.

SAVAS, O. 1987 Stability of Bödewadt flow. *J. Fluid Mech.* **183**, 77–94.

SCHLICHTING, H. 1979 *Boundary-Layer Theory*, 7th Edn. McGraw-Hill.

SCHOUVEILER, L., LE GAL, P. & CHAUVE, M.-P. 2001 Instabilities of the flow between a rotating and a stationnary disk. *J. Fluid Mech.* **443**, 329–350.

SCHOUVEILER, L., LE GAL, P., CHAUVE, M.-P. & TAKEDA, Y. 1999 Spiral and circular waves in the flow between a rotating and a stationary disk. *Exps. Fluids* **26**, 179–187.

SCHULTZ-GRUNOW, F. 1935 Der Reibungswiderstand rotierender Scheiben in Gehausen. *Z. Angew. Math. Mech.* **5**, 191–204.

SIRIVAT, A. 1991 Stability experiment of flow between a stationary and a rotating disk. *Phys. Fluids* A **3**, 2664–2671.

STÉPANOFF, A. J. 1932 Pompes centrifuges et pompes hélices. *Trans. ASME* **54**, 334–352.

STEWARTSON, K. 1953 On the flow between two rotating coaxial disks. *Proc. Camb. Phil. Soc.* **49**, 333–341.

SZERI, A. Z., SCHNEIDER, S. J., LABBE, F. & KAUFMAN, H. N. 1983 Flow between two rotating disks. Part 1. Basic flow. *J. Fluid Mech.* **134**, 103–131.